http://doi.org/10.35784/iapgos.6253

received: 24.05.2024 | revised: 03.12.2024 | accepted: 05.12.2024 | available online: 21.12.2024

AI-BASED FIELD-ORIENTED CONTROL FOR INDUCTION MOTORS

Elmehdi Benmalek, Marouane Rayyam, Ayoub Gege, Omar Ennasiri, Adil Ezzaidi

Mohammed V University in Rabat, Ecole Nationale Supérieure d'Arts et Métiers, Electronic Systems Sensors and Nanobiotechnologies, Rabat, Morocco

Abstract. *The current article deals with the implementation of Reinforcement Learning based Field Oriented Control (FOC) for the induction motors (IM). It is pertinent to mention that although conventional controllers like PID are widely used in FOC induction, they are model-based and face problems such as parameter adjustment. PID controllers need to be tuned because of the approximations of the model, variations of the parameters during operation, and the external disturbances that are uncertain and unpredictable. RL is a machine learning approach that is model-free which can adapt to the variations and disturbances. Therefore, these controllers can be an excellent alternative to the conventional controllers. In this study, an RL-based controller was used to control the speed of the induction motor using the FOC and space vector modulation (SVM). Computational simulations were done using the MATLAB/SIMULINK to test the controllers' performance under different operating conditions. This study highlights the effectiveness of RL in optimizing IM control, offering potential benefits in various industrial and automation applications.*

Keywords: induction motor, field-oriented control, NPC inverter, reinforcement learning, TD3 agent

STEROWANIE ZORIENTOWANE POLOWO DLA SILNIKÓW INDUKCYJNYCH OPARTE NA SZTUCZNEJ INTELIGENCJI

Streszczenie. *Niniejszy artykuł dotyczy implementacji uczenia ze wzmacnianiem (Reinforcement Learning – RL) opartego na sterowaniu polowym (FOC) dla silników indukcyjnych (IM). Należy wspomnieć, że chociaż konwencjonalne regulatory, takie jak PID, są szeroko stosowane w indukcji FOC, są one oparte na modelu i napotykają problemy, takie jak dostosowanie parametrów. Regulatory PID muszą być dostrajane ze względu na przybliżenia modelu, zmiany parametrów podczas pracy, oraz zewnętrzne zakłócenia, które są niepewne i nieprzewidywalne. RL to podejście oparte na uczeniu maszynowym, które jest wolne od modelu i może dostosowywać się do zmian i zakłóceń. Dlatego też regulatory te mogą być doskonałą alternatywą dla konwencjonalnych regulatorów. W niniejszym badaniu do sterowania prędkością silnika indukcyjnego wykorzystano sterownik oparty na RL, wykorzystujący FOC i modulację wektora przestrzennego (SVM). Symulacje obliczeniowe przeprowadzono przy użyciu MATLAB/SIMULINK w celu przetestowania wydajności sterowników w różnych warunkach pracy. Badanie to podkreśla skuteczność RL w optymalizacji sterowania IM, oferując potencjalne korzyści w różnych zastosowaniach przemysłowych i automatyzacji*

Słowa kluczowe: silnik indukcyjny, sterowanie polowe, przekształtnik NPC, uczenie ze wzmacnianiem, agent TD3

Introduction

Owing to their dependability and affordability, induction motors are widely used in industries [9]. Nonetheless, it can become difficult to control them particularly with respect to torque and motor speed regulation. Vector control, also known as Field Oriented Control (FOC), was thus developed to overcome such difficulties. Proposed in the 1970s by Hasse [8] and Blaschke [3], it allows for independent torque and flux control, like in a separately excited DC machine. By representing motor quantities in vector format, it ensures good performance characteristics in both the steady state as well as during dynamic conditions with good transient response. With FOC, the algorithm of control effects the transformation to the synchronous reference frame in which all the variables are expressed as DC quantities, and simplifies the control. Although direct control of induction motors (IM) in industry is commonly employed, there are limitations such as noise interference, disturbances, non-linearities and load variations [18]. Use of Artificial intelligence (AI) for direct control could address these concerns precisely and effectively. Reinforcement learning involves training a system using trial-and-error processes so that it can make decisions by itself. By selecting actions that lead to good results while avoiding an action that leads to bad ones the system learns how to maximize rewards [19]. This approach deals effectively with complex systems having multiple variables which are not well controlled through conventional techniques. This machine learning method learns on its own how best optimize performance but requires prior learning phase and may be more complicated in terms of implementation [5].

Multilevel inverters (MLIs) provide numerous advantages over conventional two-level voltage source inverters. These benefits include reduced ratings for individual devices, minimized harmonic distortion in the output voltage waveform, lower common-mode voltage, decreased dv/dt stress on power electronic components, and operation at reduced switching frequencies while maintaining the same total harmonic distortion (THD) in the output voltage [1]. Despite these advantages, MLIs also introduce several challenges, such as reduced reliability, lower efficiency, increased control complexity, and difficulties in maintaining capacitor voltage balance [2]. The three main topologies of multilevel converters are: Diode Clamped or Neutral Point Clamped, Flying Capacitor Multilevel and Cascaded H-Bridge (CHB) Multilevel [1].

The most commonly used modulation techniques for MLIs are carrier-based sinusoidal pulse-width modulation (SPWM) and space vector modulation (SVM). Of the two, SVM has several advantages, such as better utilization of the DC link voltage, more flexibility in designing the switching pattern, lower switching frequency for the power devices, and easy implementation in digital systems [1]. This makes SVM a favourite for many industrial applications. This approach, commonly referred to as SVM-FOC, helps mitigate high ripple levels despite its inherent complexity. The SVM-FOC algorithm employs linear PI controllers for torque and flux to calculate the reference control voltages [11]. Traditional mathematical models in terms of conventional analytical techniques are generally based on approximate assumptions and do not consider unmodeled dynamics. Furthermore, such models can be affected by parameter variations due to environmental conditions and/or external disturbances during operation. Consequently, linear control approaches, such as PI controllers, cannot meet the optimal performance expectations. Leveraging artificial intelligence methods to FOC of IM fed from space vector modulated converter holds the promise of improving system's performance [4].

The application of the Q-Learning algorithm to determine the optimal action for each state within the environment is introduced in [13]. In this approach, states are defined by quantized values of electromagnetic torque and motor speed, while actions are represented by magnetic current. Simulation results indicate that this method can reduce power loss by approximately 50% compared to the standard FOC motor driver when the motor operates under low loads. To attain high estimation accuracy and a compact model size, the authors have employed physically-inspired neural network structures derived from expert knowledge, rather than arbitrary topologies (a technique known as hybrid modelling) [14]. The key benefit of this method is that training the embedded neural networks requires only recorded torque measurements, without the need for additional flux measurements. Across the entire operating range, this approach achieves a root mean square torque estimation error of just 1.0% relative to the nominal torque. In contrast, using a standard open-loop current model to observe magnetic flux results in a normalized root mean square torque error of 4.6%. The design of a non-linear feedback controller for an induction motor utilizing a reinforcement learning agent is presented in [10]. The proposed controller operates using only the reference speed and the error (the difference between the reference speed and the actual output) as control inputs to generate the necessary torque, ensuring the rotor speed aligns with the reference speed. The reinforcement learning-based speed control algorithm is implemented, and the closed-loop system is thoroughly analysed. The results demonstrate that the proposed controller effectively manages the outer loop, which controls the induction motor's speed by taking various actions based on the given state. The performance of the proposed control schemes is validated under different operating conditions through simulation results. A method for generating a parameter lookup table that can achieve optimal torque across a wide range of currents and speeds, even when current commands are not set accurately is introduced in [12]. Utilizing the motor's testing data, this method employs a reinforcement learning algorithm to iteratively create the parameter lookup tables. Experimental results indicate that the proposed method can learn the appropriate parameters from operational data to produce optimal torque. Comparative studies reveal that this method can generate 5%–25% more torque than traditional model-based parameter estimation methods across various currents and speeds. Additionally, the proposed method features faster convergence and higher identification resolution compared to many conventional search-based methods.

The aim of this paper is to design and simulate FOC for the IM fed from space vector modulated inverter using reinforcement learning. To evaluate the performances of the proposed method, we simulating different conditions: adding a load, changing the speed and then inversing it to evaluate how well the system adapt to different real-world scenarios. The simulations were done using MATLAB/SIMULINK and Reinforcement learning toolbox.

1. Space vector modulation

In the FOC strategy, SPWM is replaced by SVM for selecting voltage vectors. This approach maintains a constant switching frequency, effectively addressing the issue of high torque and phase current ripples—a key limitation of conventional FOC. SVM, first introduced in the late 1980s as an alternative to basic PWM, has since undergone extensive development in both theory and practical implementation. SVM is based on the space vector representation of the voltage output from the inverter. Unlike conventional PWM, it does not use separate modulators for each phase. Instead, reference voltages are expressed as a space voltage vector, representing voltage components in the complex plane. The core principle of SVM involves predicting the inverter voltage vector by projecting the reference vector onto the two adjacent vectors corresponding to two active switching states [17].

Based on inverter level, the switching vectors form a hexagonal diagram divided into six sectors, each spanning 60°, as illustrated in Figure 1. SVM offers several advantages, including reduced ripple, lower THD, and minimized switching losses [15].

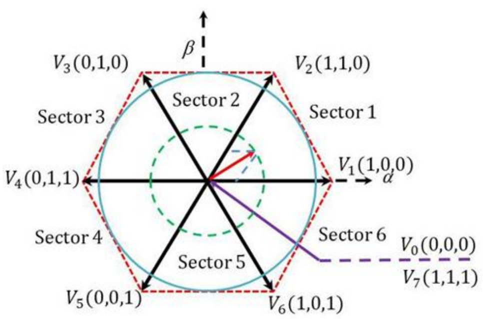

Fig. 1. Diagram of voltage space vector

The application time for each vector is determined through vector calculations, with any remaining time within the switching period allocated to the null vector. For instance, when the reference voltage lies in sector 1, as illustrated in Figure 2, it can be synthesized by combining the vectors V_1, V_2 and V_0 (the zero vector) [7].

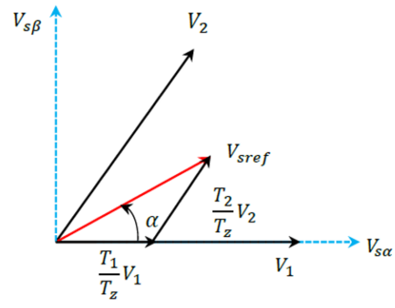

Fig. 2. Reference vector as a combination of adjacent vectors at sector 1

The volt-second balance principle for sector 1 can be represented as:

$$V_s^* T_z = V_1 T_1 + V_2 T_2 + V_0 T_0 \tag{1}$$

$$T_z = T_1 + T_2 + T_0 \tag{2}$$

The application times for the voltage vectors, T_1, T_2, and T_0, correspond to their respective durations within the sampling period T_z. The values of T_1 and T_2, associated with the voltage vectors, are determined through straightforward projections.

$$T_1 = \frac{T_z}{2V_{dc}}\left(\sqrt{6}V_{s\beta}^* - \sqrt{2}V_{s\alpha}^*\right) \tag{3}$$

$$T_2 = \frac{\sqrt{2}T_z}{V_{dc}} V_{s\alpha}^* \tag{4}$$

Using V_{dc}, the DC bus voltage, the switching times (duty cycles) can be calculated as follows [21, 22]. Figure 3 illustrates this process, while Table 1 provides a summary of the switching times (outputs) for each sector.

$$T_{a_{on}} = \frac{T_z - T_1 - T_2}{2} \tag{5}$$

$$T_{b_{on}} = T_{a_{on}} + T_1 \tag{6}$$

$$T_{c_{on}} = T_{b_{on}} + T_2 \tag{7}$$

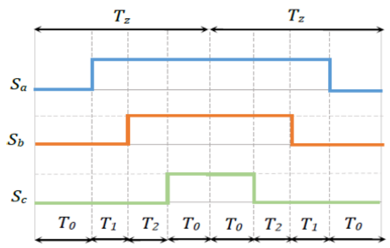

Fig. 3. Switching times of sector 1

Table 1. Switching times for each sector

Sector	1	2	3	4	5	6
S_a	$T_{b_{on}}$	$T_{a_{on}}$	$T_{a_{on}}$	$T_{c_{on}}$	$T_{b_{on}}$	$T_{c_{on}}$
S_b	$T_{a_{on}}$	$T_{c_{on}}$	$T_{b_{on}}$	$T_{b_{on}}$	$T_{c_{on}}$	$T_{a_{on}}$
S_c	$T_{c_{on}}$	$T_{b_{on}}$	$T_{c_{on}}$	$T_{a_{on}}$	$T_{a_{on}}$	$T_{b_{on}}$

2. Modeling of the induction motor

The equivalent IM model is a simplified representation of the motor using mathematical equations [16]. These equations were used to describe motor's behavior in relation to current, voltage, torque and speed. This model is commonly employed in simulation studies and designing control systems [6]. The parameters of these models are usually obtained from experimental measurements or provided by motor manufacturers. Among these parameters there are stator phase resistance R_s and rotor phase resistance R_r, stator phase inductance L_s and rotor phase inductance L_r, the mutual inductance L_m and the electrical time constant τ.

2.1. Voltage equations

The matrices below summarize the 3 stator flow equations:

$$\begin{bmatrix}\phi_{as}\\ \phi_{bs}\\ \phi_{cs}\end{bmatrix}=\underbrace{\begin{bmatrix}L_s & M_s & M_s\\ M_s & L_s & M_s\\ M_s & M_s & L_s\end{bmatrix}}_{[L_{ss}]}\begin{bmatrix}I_{as}\\ I_{bs}\\ I_{cs}\end{bmatrix}+M\underbrace{\begin{bmatrix}\cos(\theta) & \cos\left(\theta-\frac{4\pi}{3}\right) & \cos\left(\theta-\frac{2\pi}{3}\right)\\ \cos\left(\theta-\frac{2\pi}{3}\right) & \cos(\theta) & \cos\left(\theta-\frac{4\pi}{3}\right)\\ \cos\left(\theta-\frac{4\pi}{3}\right) & \cos\left(\theta-\frac{2\pi}{3}\right) & \cos(\theta)\end{bmatrix}}_{[M_{sr}]}\begin{bmatrix}I_{ar}\\ I_{br}\\ I_{cr}\end{bmatrix} \quad (8)$$

In a similar way, the rotor flow equations:

$$\begin{bmatrix}\phi_{ar}\\ \phi_{br}\\ \phi_{cr}\end{bmatrix}=\underbrace{\begin{bmatrix}L_r & M_r & M_r\\ M_r & L_r & M_r\\ M_r & M_r & L_r\end{bmatrix}}_{[L_{rr}]}\begin{bmatrix}I_{ar}\\ I_{br}\\ I_{cr}\end{bmatrix}+M\underbrace{\begin{bmatrix}\cos(\theta) & \cos\left(\theta-\frac{2\pi}{3}\right) & \cos\left(\theta-\frac{4\pi}{3}\right)\\ \cos\left(\theta-\frac{4\pi}{3}\right) & \cos(\theta) & \cos\left(\theta-\frac{2\pi}{3}\right)\\ \cos\left(\theta-\frac{2\pi}{3}\right) & \cos\left(\theta-\frac{4\pi}{3}\right) & \cos(\theta)\end{bmatrix}}_{[M_{rs}]}\begin{bmatrix}I_{as}\\ I_{bs}\\ I_{cs}\end{bmatrix} \quad (9)$$

$$[V_s]=R_s[I_s]+\frac{d}{dt}([L_{ss}][I_s])+\frac{d}{dt}([M_{sr}][I_r]) \quad (10)$$

$$[0]=R_r[I_r]+\frac{d}{dt}([L_{rr}][I_r])+\frac{d}{dt}([M_{rs}][I_s]) \quad (11)$$

2.2. Mechanical equations

The characteristics of the induction machine include the electrical parameters (voltage, current, flux) and the mechanical ones (torque, speed) [6].

$$\begin{cases} C_e=p[I_s]^t[M_{sr}][I_r]\\ J\frac{d}{dt}\Omega=C_e-C_r-k_f\Omega\end{cases} \quad (12)$$

J – moment of inertia of the rotating masses, C_r – resistant torque applied to the machine shaft, C_e – electromagnetic torque, Ω – rotor electrical speed, K_f – viscous friction coefficient.

2.3. State equations

An IM has the stator voltages V_{sd} and V_{sq} as control variables and as a disturbance the resisting torque C_r. Several state variables can describe the IM [6]. In our study, it will be represented by the stator currents and the rotor fluxes ($I_{ds}, I_{qs}, \varphi_{dr}, \varphi_{qr}$).

The mathematical model is in the form:

$$[\dot{X}]=[A][X]+[B][U] \quad (13)$$

where:

$[X]$ – state vector, $[i_{ds}, i_{qs}, \Phi_{ds}, \Phi_{qs}]^T$, $[U]$ – command vector $[V_{ds}, V_{qs}, 0, 0]^T$, $[A], [B]$ – matrices related to flow control.

The IM model in the form of an equation of state in a frame of reference linked to the rotating field can be written as follows:

$$\left\{\begin{array}{l} \frac{d}{dt}i_{ds}=\frac{1}{\sigma.L_s}\left[V_{ds}-\left(R_s+\frac{M^2R_r}{L_r^2}\right)I_{ds}+\sigma L_s\omega_s i_{qs}+\frac{M}{T_rL_r}\varphi_{dr}+\omega_r\frac{M}{L_r}\varphi_{qr}\right]\\ \frac{d}{dt}i_{qs}=\frac{1}{\sigma.L_s}\left[V_{qs}-\left(R_s+\frac{M^2R_r}{L_r^2}\right)I_{qs}+\sigma L_s\omega_s i_{ds}+\frac{M}{T_rL_r}\varphi_{qr}+\omega_r\frac{M}{L_r}\varphi_{dr}\right]\\ \frac{d}{dt}\varphi_{dr}=\frac{M}{T_r}I_{ds}-\frac{1}{T_r}\varphi_{dr}+\omega_s\varphi_{qr}\\ \frac{d}{dt}\varphi_{qr}=\frac{M}{T_r}I_{qs}-\frac{1}{T_r}\varphi_{qr}+\omega_s\varphi_{dr}\\ C_{em}=\frac{pM}{L_r}(\varphi_{dr}I_{qs}-\varphi_{qr}I_{ds})\\ \frac{d\Omega}{dt}=\frac{1}{J}C_{em}-\frac{C_r}{J}-\frac{K_f}{J}\Omega \end{array}\right. \quad (14)$$

with: $\sigma=1-\frac{L_m^2}{L_sL_r}$ equals the Dispersion Coefficient.

3. Field-oriented control by reinforcement learning

RL applied to direct control of induction motors is a novel approach in this field. The method employs machine learning techniques to dynamically adjust control parameters that improve the efficiency, performance and responsiveness of engine. It differs from traditional methods because it automatically adapts to changes in load and operating conditions thereby potentially increasing energy efficiency as well as reducing maintenance costs. The FOC for IM diagram is shown in Fig. 4. This section expounds on the principles and benefits associated with this emerging technology in IM control.

- Automated decision-making (for actions and/or control) within a complex domain with unclear constraints.
- Learning through experience, establishing a behavioral strategy (known as policy) based on observed failures or successes (reinforcements or rewards).

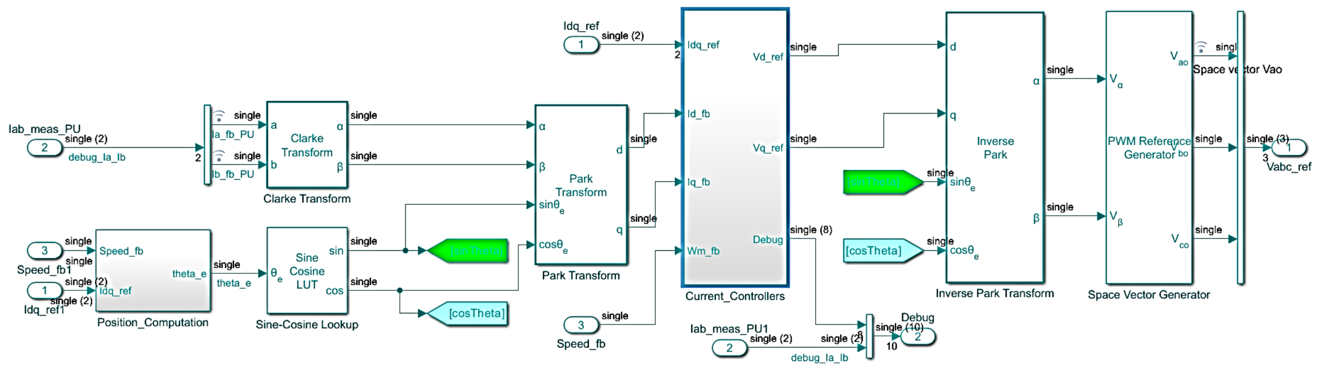

Fig. 4. Field-oriented control for induction motors

3.1. The RL agent

We used RL agent to replace the regulators of direct and quadrature currents by using vector control with speed regulation and cascaded current control; thus, making significant step closer towards self-controlled adaptive motor. The RL agent decides which actions including modulation voltage or changing some of the controlling parameter depending on the information received, it then chooses those actions having higher values of rewards. The model was developed for optimization purposes when transferring into an RL agent so that real-time optimization can improve motor performance, by adapting the control to load variations. The RL agent learns the behavior of our control system and provides corrective signals for the system after the learning phase.

3.2. Insertion of RL

We replaced the PI corrector of the internal loop of the quadrature and direct currents with the RL block (Fig. 5), which includes other components (observations, rewards, and the RL agent).

- RL Agent: to be trained,
- Reward: the function for calculating rewards for the RL agent,
- Observations: the states of the environment observed by the RL agent,
- Action: the output provided by the RL agent.

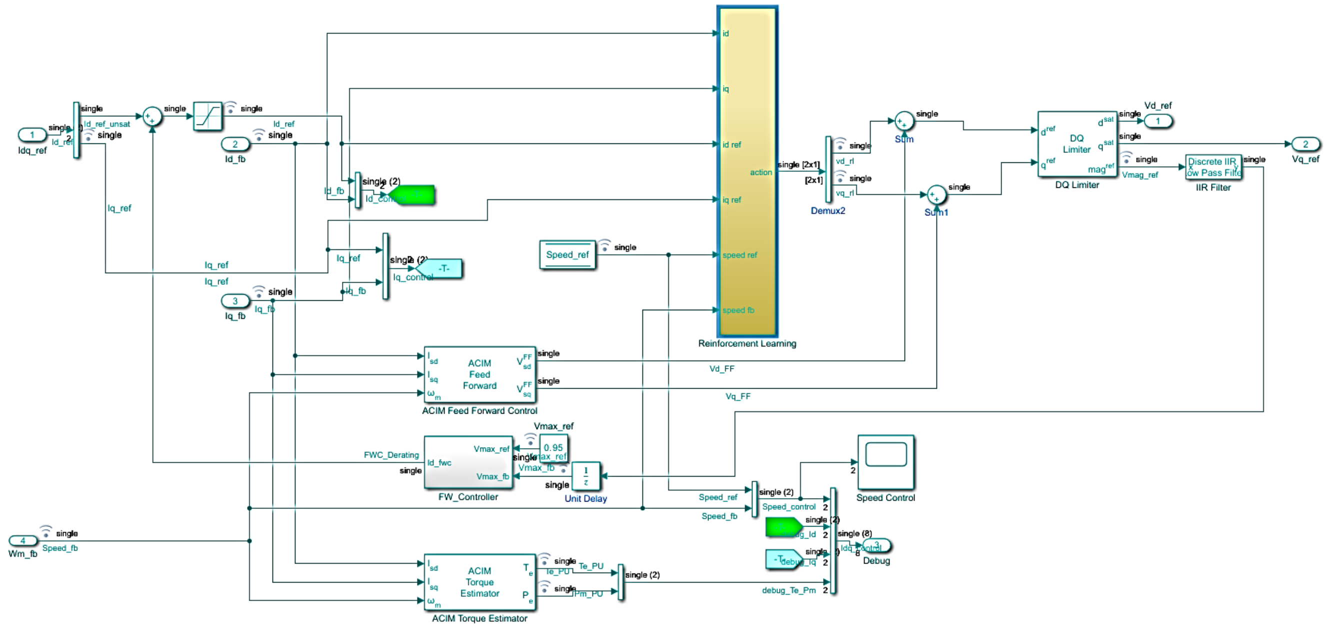

Fig. 5. Control loop using the RL

3.3. State observations

This block represents data gathered from the environment by an agent, which gives information on the behaviour of the system usually in form of data or variables that are relevant to the agents decision-making process. For this step, we will use our Simulink diagram to create our own state observer. In our case, IM speed will be included as well as integration of I_d and I_q current errors in order to have our state observer.

3.4. Reward function

In this step, our function assigns a numerical value to each action taken by an agent. It guides the agent towards desired behaviors by favoring beneficial actions and penalizing undesirable actions. The reward function utilized is as follows:

$$r_t = -\left(5 i_{d\,error}^2 + 5 i_{q\,error}^2 + 0.1 \sum_i \left(u_{t-1}^j\right)^2\right) - 100d \qquad (15)$$

with the parameters:

$\left(u_{t-1}^j\right)$ – previous step actions,

d – an indicator that equals 1 if the simulation is finished so early.

We observe that the reward is determined based on the quadratic reward penalty, which penalizes the deviation from the optimal control. The block diagram in Simulink for the reward block is presented in Fig. 6.

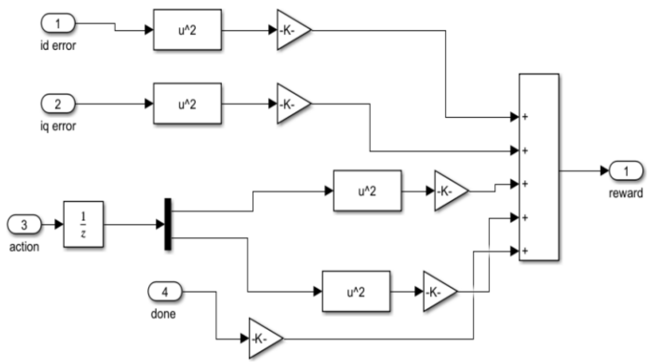

Fig. 6. Block diagram of the reward function

3.5. Creation of RL Agent

Before the training of the agent, it is necessary to configure the parameters of our algorithm utilizing deep neural networks, commonly referred to as deep reinforcement learning (DRL).

We choose hyperparameters for Twin Delayed Deep Deterministic Policy Gradient (TD3) agent such as learning rate, degradation factor, exploration parameters. These parameters have much effect on how the agent learns and explores its environment with aim to perfecting its action policy. Fig. 7 represents the block diagram of the agent, as the Fig. 8 shows different options used for its configuration.

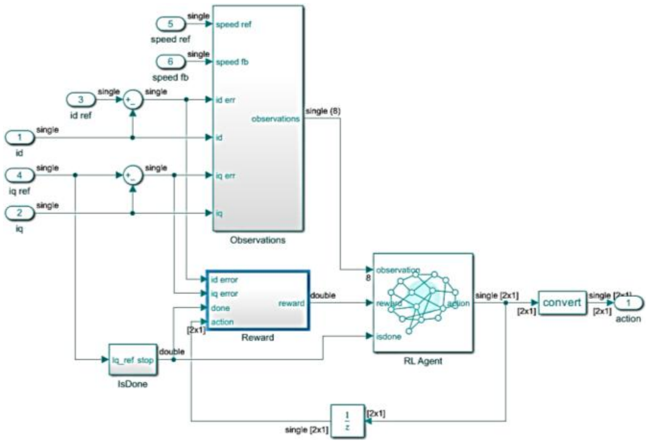

Fig. 7. RL Agent block diagram

```
agentOpts =
  rlTD3AgentOptions with properties:

                 ExplorationModel: [1x1 rl.option.GaussianActionNoise]
           TargetPolicySmoothModel: [1x1 rl.option.GaussianActionNoise]
             PolicyUpdateFrequency: 2
             ActorOptimizerOptions: [1x1 rl.option.rlOptimizerOptions]
            CriticOptimizerOptions: [1x2 rl.option.rlOptimizerOptions]
                TargetSmoothFactor: 0.0050
             TargetUpdateFrequency: 10
ResetExperienceBufferBeforeTraining: 1
                    SequenceLength: 1
                     MiniBatchSize: 1012
               NumStepsToLookAhead: 1
            ExperienceBufferLength: 2000000
                        SampleTime: 0.0565
                    DiscountFactor: 0.9950
                        InfoToSave: [1x1 struct]
```

Fig. 8. TD3 Agent Options

The first step is to define the observations that can be made by an agent from its environment and also the actions it can do. This configuration shows how far the agent can go in interacting with its environment. We construct two neural networks that will be used as the actor (decision making) as well as critic (evaluating actions) for this interaction. The critic network has two entry points (for observations and actions) and outputs estimation of Q function. The actor network takes input from observations and produces output on what action to take. The learning rate for actors is 1e-3, gradient threshold equals 1 while L2 regularization factor is 1e-3 for critics.

4. Results

Agent learning step involves training it using TD3 algorithm in RL framework. The agent learns to make decisions based on an actor-critic model through maximizing accumulated rewards while refining its action policy. Here are the training parameters: Each training session is a set of 1000 episodes, each consisting of 5000 steps, and the mini-batch size is 512. To encourage long term gains we use a discount factor of 0.995. Our training will stop when the evaluation average cumulative reward surpasses -75. This means that the agent can follow reference speeds. The learning graph is presented in Fig. 9.

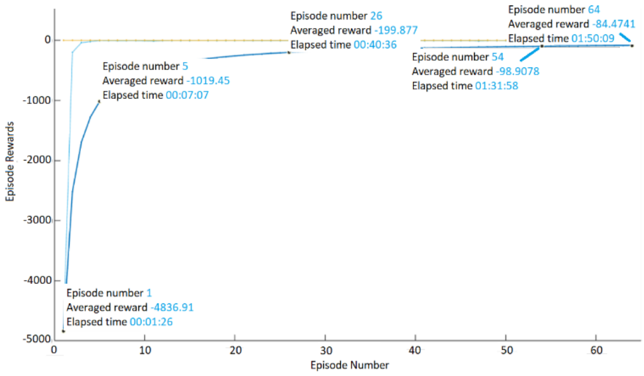

Fig. 9. RL training progression

In Fig. 10, we tested our model before it finishes learning. The performance for our IM control model is shown which demonstrates its current state as not fully optimized. However, these results provide insights about the capabilities and behaviour of this model. The performance of the RL based IM control during training, the agent learned to follow the reference but still did not capture all dynamics, especially when the speed is inverted.

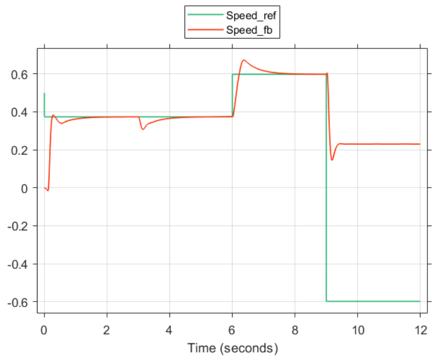

Fig. 10. Speed response while RL training

The performance of the RL based IM control is shown in Fig. 11. the agent learned to follow the reference even when we inverted the speed, meaning the agent learns the system dynamics with time. At 3-seconds mark, a load was introduced thus activating RL algorithm to adapt its motor control strategies to meet higher demands in terms of power supply needed by loads put on it hence requiring more power inputs to keep track with load changes. By the 6-second mark, the model increase speed reacting to the demand. Furthermore, at the 9-second mark, the algorithm followed the reference when we inverted the motor speed, indicative of its robustness in handling complex control scenarios. The tracking error remains zero in the 3 applied disturbances. The motor delay time in the start is 0.6 second, 1 second when the extra load being added. When increasing and then decreasing speed of the motor, the settling time is 0.5 second and 1 second respectively. It should be noted that overshoot percentage is 5% for motor initiation, 13% during load application, for speed increase 4%, while speed reversal 5%. When it comes to the disturbance resilience, our model consistently returns back to the reference state after disturbances, proving our model robustness. This evaluation highlights the effectiveness of RL in optimizing IM control, offering potential benefits in various industrial and automation applications.

In Fig. 12, we present the direct and quadrature currents I_d and I_q, which are essential parameters for assessing performance of our IM control system. These currents help us understand how well our motor operates as well as its efficiency. By monitoring these quantities, we can evaluate how effectively the system manages torque and flux of a motor ensuring an optimal operating condition. Visualizing the I_d and I_q, provide important information regarding whether our control strategy is effective and whether the motor works stably and efficiently or not. Our model track both currents when a load is added and speed increased, but there is a brief disturbance of the direct current during reversal of speed.

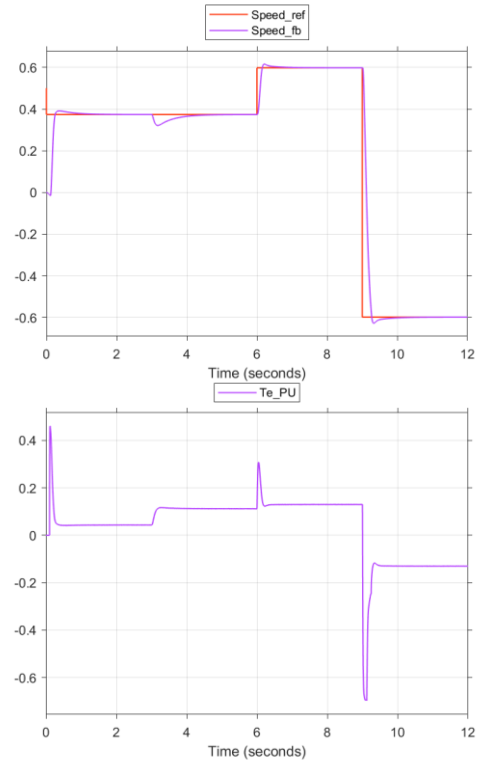

Fig. 11. Speed and torque response

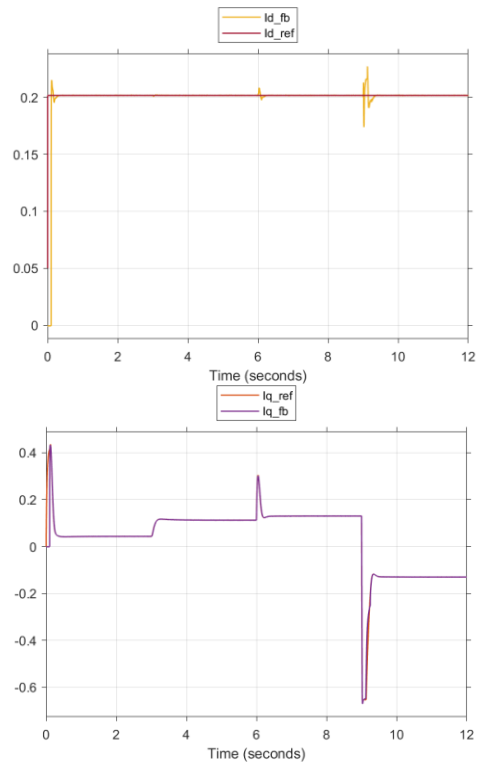

Fig. 12. Courants I_d and I_q responses

Figure 13 compares voltage V_a against its homologue obtained through SVM at the 3-second, 6-second, and 9-second marks. This enables us to have a clear view on how effective this particular modulation technique controls the motor. Through comparing V_a which is reference voltage with actual voltage generated via SVM, this can provide us with insights regarding accuracy for modulation and closeness of system in tracking the required voltage waveform. Assessment of the interconnection between these two signals helps in evaluating SVM algorithm efficacy as well as assessing its impact on motor efficiency and dynamic response.

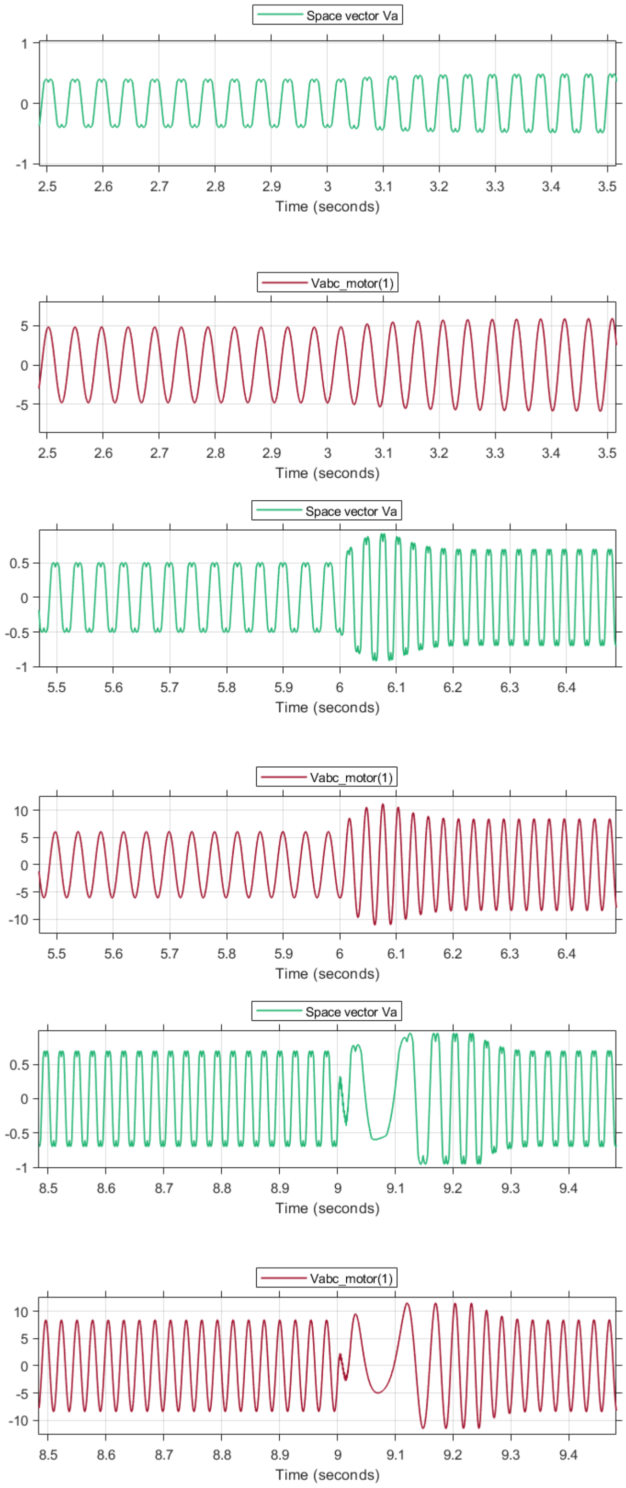

Fig. 13. Comparison of V_a (in red) and its homologue in space vector modulation (in green)

5. Disscussion

RL has several advantages as opposed to traditional control methods. One major advantage is its adaptability to the dynamic and uncertain environment without requiring a precise model of the system dynamics. RL's ability to learn from experience enables it to keep improving continuously over time, thus making it highly relevant in changing environments or tasks. However, when compared with conventional control approaches, RL algorithms require a large amount of data and exploration for learning effective policies. In some cases, this can be inefficient especially in systems where data collection is expensive or time-consuming as opposed to classical control approaches that might involve mathematical models or heuristics. The RL can be computationally demanding, requiring considerable computational resources and training time particularly in high-dimensional or continuous action spaces. Moreover, these RL models are sensitive to uncertainties in their environment and may fail at generalizing over unseen scenarios or noisy data. They also need to balance between exploration (trying new actions in order to find better policies) and exploitation (doing what we already know is best). In safety-critical applications, RL algorithms might exhibit unstable or unsafe behavior during learning, which is problematic.

A range of factors must be taken into account when implementing RL such as reward design, hyperparameter tuning, environment setup and training infrastructure. Nonetheless, RL holds considerable promise in domains with complex dynamics but its limitations must be addressed. Therefore, addressing these limitations and developing more robust RL algorithms are still active research areas. The full potential of RL in optimizing IM control in industrial and automation applications can be realized if scalable RL algorithms and methodologies tailored to electrical machines are developed by researchers involved in this area.

6. Conclusions

This paper aims to investigate controlling of an IM through a space vector modulated inverter using RL. This AI technique can adapt well to changing environments and optimize over time, which suggest that the model has potential advantages in terms of adaptation and performance optimization for more complex dynamic systems compared to vector control with PI controller. This study highlights the effectiveness of RL in optimizing IM control, offering potential benefits in various industrial and automation applications. Finally, the selection between these methods will have to be based on specific application requirements and objectives. Our paper detailed the implementation of RL in motor control thus enabling future work in regard to sophisticated applications for controlling IM.

Statements and declarations

The authors declare no competing interests.

References

[1] Balal A. et al.: A review on multilevel inverter topologies. Emerging Science Journal 6(1), 2022, 185–200.
[2] Barzegarkhoo R. et al.: Switched-capacitor multilevel inverters: A comprehensive review. IEEE Transactions on Power Electronics 37(9), 2022, 11209–11243.
[3] Blaschke F.: The principle of field orientation as applied to the new transvector closed-loop system for rotating-field machines. Siemens Review 34(3), 1972, 217–220.
[4] Chinmaya K. A., Singh G. K.: Experimental analysis of various space vector pulse width modulation (SVPWM) techniques for dual three-phase induction motor drive. International Transactions on Electrical Energy Systems 29(1), 2019, e2678.
[5] Ding Z. et al.: Introduction to reinforcement learning. Deep reinforcement learning: fundamentals, research and applications, 2020, 47–123.

[6] Goolak S. et al.: Mathematical modeling of an induction motor for vehicles. Eastern-European Journal of Enterprise Technologies 2(2), 2020, 104.
[7] Hari V., Narayanan G.: Space-vector-based hybrid pulse width modulation technique to reduce line current distortion in induction motor drives. IET Power Electronics 5(8), 2012, 1463–1471.
[8] Hasse K.: On the dynamics of speed control of a static ac drive with a squirrel-cage induction machine. Ph.D., TH Darmstadt, 1969.
[9] Kumar P., Hati A. S.: Review on machine learning algorithm based fault detection in induction motors. Archives of Computational Methods in Engineering 28, 2021, 1929–1940.
[10] Memon A. Y.: Reinforcement Learning Based Field Oriented Control Of An Induction Motor. Third International Conference on Latest trends in Electrical Engineering and Computing Technologies (INTELLECT). Pakistan, Karachi, 2022, 1–8.
[11] Patel P. J., Patel V., Tekwani P. N.: Pulse-based dead-time compensation method for self-balancing space vector pulse width-modulated scheme used in a three-level inverter-fed induction motor drive. IET Power Electronics 4(6), 2011, 624–631.
[12] Qi X., Cao W., Aarniovuori L.: Reinforcement learning based parameter lookup table generating method for optimal torque control of induction motors. IEEE Transactions on Industrial Electronics 70(5), 2022, 4516–4525.
[13] Sistani M. B. N., Hesari S.: Decreasing Induction Motor Loss Using Reinforcement Learning. Journal of Automation and Control Engineering 4(1), 2016.
[14] Stender M., Wallscheid O., Böcker J.: Accurate torque estimation for induction motors by utilizing a hybrid machine learning approach. IEEE 19th International Power Electronics and Motion Control Conference (PEMC). 2021, 390–397.
[15] Tamilvani M. et al.: Harmonic reduction in variable frequency drives using active power filter. Bulletin of Electrical Engineering and Informatics (BEEI) 3(2), 2014, 119–126.
[16] Torrey D. A., Selamogullari U. S.: Modelica implementation of field-oriented controlled 3-phase induction machine drive. 2nd Int. Modelica Conf., DLR, Oberpfaffenhofen, Germany 2002, 173–182.
[17] Vaezi S. A., Iman-Eini H., Razi R.: A New Space Vector Modulation Technique for Reducing Switching Losses in Induction Motor DTC-SVM Scheme. 10th International Power Electronics, Drive Systems and Technologies Conference (PEDSTC). Iran, Shiraz, 2019, 184–188.
[18] Wang F. et al.: Advanced control strategies of induction machine: Field oriented control, direct torque control and model predictive control. Energies 11(1), 2018, 120.
[19] Wang H. N. et al.: Deep reinforcement learning: a survey. Frontiers of Information Technology & Electronic Engineering 21(12), 2020, 1726–1744.
[20] Zahraoui Y., Akherraz M., Fahassa C.: Induction Motor DTC Performance Improvement By Reducing Torque Ripples in Low Speed. U.P.B. Sci. Bull., Series C 81(3), 2019, 249–260.
[21] Zhang Z. et al.: Novel Direct Torque Control Based on Space Vector Modulation With Adaptive Stator Flux Observer for Induction Motors. IEEE Transactions on Magnetics 46(8), 2010, 3133–3136.

Ph.D. Elmehdi Benmalek
e-mail: elmehdi.benmalek@um5s.net.ma

Received his Ph.D. from Mohammed V University in Rabat in 2019.
His research interests include signal processing, embedded systems and machine learning.

https://orcid.org/ 0000-0003-1078-1421

Prof. Marouane Rayyam
e-mail: 03malaho06@gmail.com

He is a professor in Mohammed V University in Rabat where he received his Ph.D. in 2021.
His research interests include motor drive, control systems and power electronics.

https://orcid.org/0000-0002-7071-8953

M.Sc. Ayoub Gege
e-mail: khokhada@gmail.com

Received his Master degree from Mohammed V University in Rabat in 2023.
His research interests include motor drive and control systems.

https://orcid.org/0009-0009-7757-1964

M.Sc. Omar Ennasiri
e-mail: khobzkarm13@gmail.com

He is a Ph.D. student in Mohammed V University in Rabat.
His research interests include energy harvesting, IoT and machine learning.

https://orcid.org/0009-0007-3656-101X

M.Sc. Adil Ezzaidi
e-mail: khobzkarm@gmail.com

He is a Ph.D. student in Mohammed V University in Rabat.
His research interests include signal processing, embedded systems and machine learning.

https://orcid.org/0009-0004-4960-0784